Materials Letters, Volume 231, 15 November 2018, Pages 159-162
DOI:10.1016/j.matlet.2018.08.046

Nitrogen-doped micropores binder-free carbon-sulphur composites as the cathode for long-life lithium-sulphur batteries

Yuechao Yao[a], Peng Liu[a], Qi Zhang[b], Shaozhong Zeng[a], Shuangshuang Chen[a], Guangjin Zou[a], Xiaohua Li[a], Xierong Zeng[a,c], Jizhao Zou[a,c]*.

[a]Shenzhen Key Laboratory of Special Functional Materials & Shenzhen Engineering Laboratory for Advance Technology of ceramics, College of Materials Science and Engineering, Shenzhen University, Shenzhen, 518060. P.R. China

[b]School of Aerospace, Transport and Manufacturing, Cranfield University, Cranfield, Bedfordshire, MK43 0AL, UK

[c] Guangdong JANUS Intelligent Group Corporation Limited, Dongguan，China

* Corresponding author. E-mail address: zoujizhao@szu.edu.cn (J.Z. Zou)

Abstract

Nitrogen-doped micropore-contained carbon nanofibres (NMCNFs) were prepared by carbonizing ZIF-8 grown in liquid-phase along with electrospinning. When NMCNFs act as sulphur host materials in lithium–sulphur batteries, NMCNFs can retard the shuttle effect and dissolution of polysulfides through the synergic action of effective physical confinement to micropores and nitrogen surface chemical absorption. NMCNFs show a capacity up to 636 mAh g^{-1} after 500 cycles against Li anode.

Keywords: Lithium-sulphur batteries, long life, binder-free cathode

1 Introduction

Lithium-sulphur batteries with high theory capacity (1675 mAh g^{-1}) have been a focus of research owing to element sulphur being cheap, abundant, environmental friendly [1]. However, some serious questions are deeply restricting the application of lithium-

sulphur batteries. Firstly, element sulphur has low conductivity (5.0×10^{-30} S·cm^{-1}) and its discharge products (Li_2S, Li_2S_2) are insulated too; secondly, the reaction intermediates, lithium polysulfides (LiS_n), are highly soluble in organic electrolytes and are easily reduced on the lithium-anode surface; Thirdly, the sulphur expansion/contraction (~80%) in charge-discharge process against lithium results in the disconnection of electrode material with current collector [2, 3], which will lead to fast capacity decay and unstable coulombic efficiency.

Carbon nanofibres (CNFs) are good sulphur hosts because of their excellent conductive network and binder-free characterises. Polyacrylonitrile (PAN)-based CNFs have high spinnability, high carbon yield, and high nitrogen doped with nitrile groups [4]. However, the low specific surface area of PAN-based porous CNFs commonly cannot be used as an effective sulphur host material because of lacking the sites for the absorption of sulphur/polysulfides. Thus, the obtained nitrogen-doped nanoporous flexible carbon nanofibres for sulphur host materials are highly desired.

In this paper, we prepared high SSA nitrogen-doped micropore flexible carbon nanofibres (NMCNFs) by electrospinning ($ZnBr_2$/PAN nanofibres) and liquid phase growth (ZIF-8/$ZnBr_2$/PAN nanofibres), followed by pyrolysis process. Furthermore, the NMCNFs/S composites were synthesized via vapour diffusion of commercial sulphur powder. The electrochemical properties of the NMCNFs/S samples were also investigated as promising electrodes for lithium-sulphur batteries.

2 Experimental

2.1 The synthesis of NMCNFs.

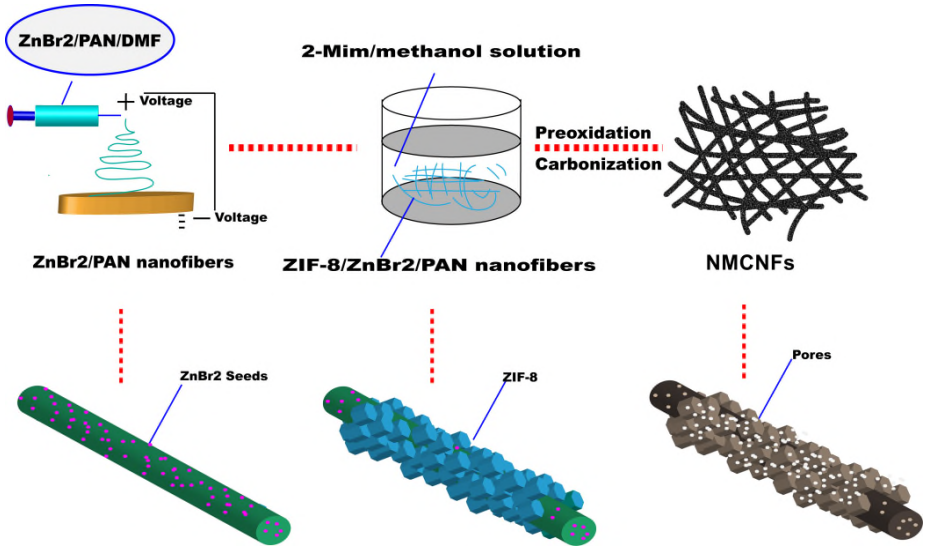

Fig. 1 Schematic illustration of the NMCNFs preparation process.

The fabrication process for high SSA nitrogen-doped micropore flexible carbon nanofibres (NMCNFs) is illustrated schematically in Fig. 1. The $ZnBr_2$/PAN composite nanofibres were synthesized by electrospinning. The 2.2 g $ZnBr_2$ particles were dispersed in 4 ml N, N-dimethylformamide by sonication. Polyacrylonitrile was completely dissolved in 7 ml DMF solution with a vigorous stirring at room temperature. Then, these two solutions were mixed and stirred for 24 h at room temperature. The 2.3 g sheet-type $ZnBr_2$/PAN nanofibres were dipped into a mixed solution of 2-methylimidazole (13 g) and methanol (400 ml) for 3 days. The obtained ZIF-8/$ZnBr_2$/PAN nanofibres were washed twice by methanol. Afterwards, ZIF-8/$ZnBr_2$/PAN nanofibres were left in air at 220 °C for 180 min and subsequently carbonized under Ar flow at 900 °C for 2 h with a rate of 5 °C min^{-1}.

2.2 The synthesis of NMCNFs/S composites.

The obtained high SSA NMCNFs were cut into electrodes (ϕ=15mm). Then, the NMCNFs/S cathodes were synthesized via vapour diffusion of commercial sulphur powder. Firstly, the NMCNFs nanosheet and sulphur was sealed in a glass bottle and

heated to 200°C at a heating rate of 2 °C/min in an oven and maintained at 200 ºC for 4 h (sulphur and NMCNFs are separated). Then, the temperature was raised to 250 °C and maintained 2 h.

2.3 The fabrication of electrode and electrochemical measurements

The obtained NMCNFS cathodes were used after being dried at 60 °C for 12 h under vacuum. The loading amount of sulphur is about 1.5-2.0 mg/cm^2 in a cell and the amount of electrolyte is 30 μL/mg S. The charge-discharge tests were conducted on NEWARE instruments with voltage window of 1.5~3.0 V versus Li^+/Li. Cyclic voltammetry (CV) experiment was performed on a CHI 660E electrochemical workstation at a scan rate of 0.2 mV/s from 3.0 to 1.5 V. The frequency range is from 10^5 to 0.05 Hz and the perturbation amplitude was 5 mV.

3 Results and discussion

Fig. 2a shows that $ZnBr_2$ is evenly anchored in PAN nanofibres as ZIF-8 seeds. As shown in the Fig. 2b, the ZIF-8/$ZnBr_2$/PAN nanofibres are successfully synthesized and the polyhedrons of ZIF-8 are fully distributed in the outer surface of $ZnBr_2$/PAN nanofibres.

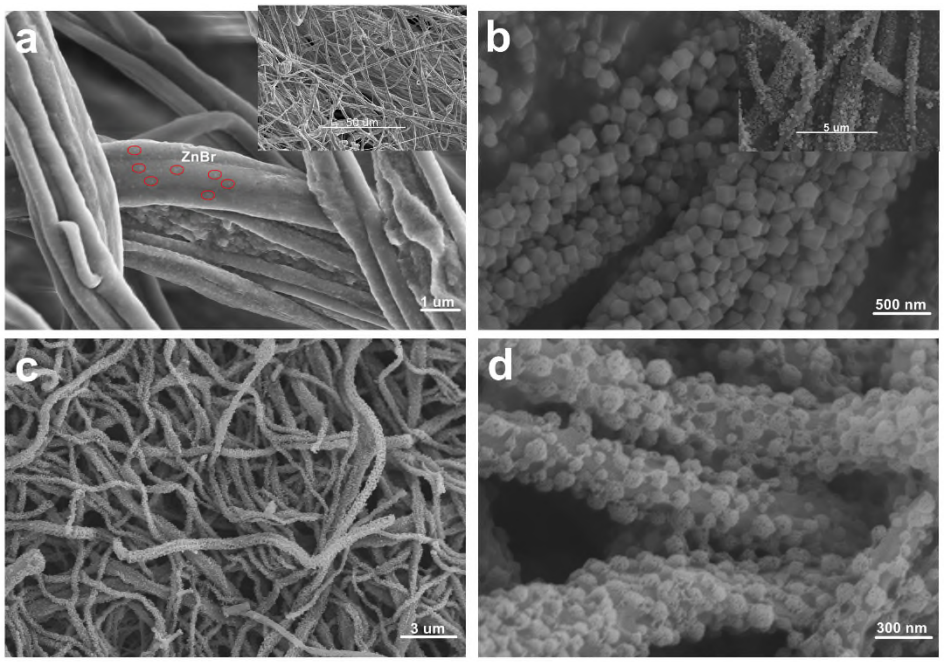

Fig. 2 Field emission scanning electron microscopy (FESEM) image of (a) $ZnBr_2$/PAN nanofibres, (b) ZIF-8/$ZnBr_2$/PAN nanofibres, (c-d) NMCNFs.

After pre-oxidation and pyrolysis process, the NMCNFs were obtained (Fig.2c-d). Fig. 2 c shows that the diameter of NMCNFs is relatively uniform, and Fig. 2d shows the ZIF-8-derived nanopores on the surface of carbon nanofibres.

The NMCNFs show a high BET surface area (693.64 m^2g^{-1}), and the total pore volume and average pore diameter are 0.36 cm^3g^{-1} and 0.72 nm respectively. Fig. 3a indicates the existence of many micropores. It has been reported that micropores could effectively absorbed chain polysulfide [5-7].

The microstructure of NMCNFs/S composites was investigated by X-ray diffraction (Fig. 3b). A weak peak of crystalline sulphur can be observed, except for peaks of NMCNFs at ~24° and ~44° in the XRD pattern correspond to the (0 0 2) and (1 0 0) diffractions of carbon materials. The result demonstrates that sulphur is uniformly distributed in the NMCNFs.

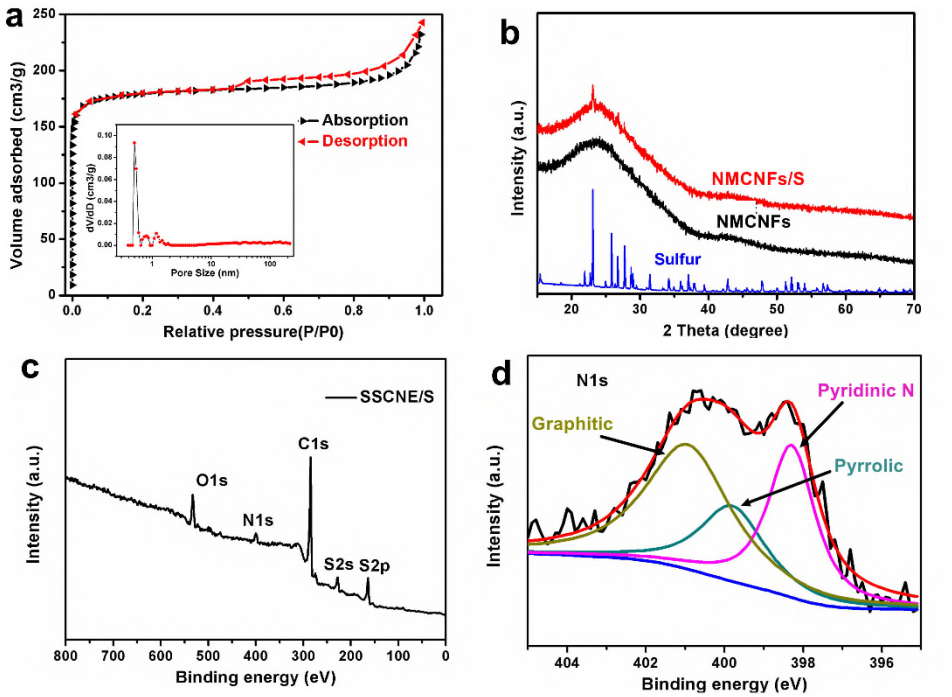

Fig. 3 (a) N_2 adsorption-desorption isotherms for NMCNFs and inset of pore diameter distribution (b) X-ray diffraction patterns of sulphur, NMCNFs and NMCNFs/S. (c) XPS spectra of NMCNFs/S . (d) NMCNFs/S high-resolution XPS spectra of the deconvoluted N 1s peak.

Fig. 3c shows that there are five obvious peaks that correspond to C1s, N1s, O1s, S2p and S2s. The high resolution N1s XPS spectrum (Fig. 3d) is divided into quatemary-N (401.1 eV), pyrrolic-N (399.8 eV), and pyridinic-N (398.3 eV), respectively [8]. Because pyrrolic-N and pyridinic-N have a lone pair of electrons and high electronegativity, they take an effective absorption of polysulfides [9, 10].

Fig. 4a shows the CV curves. In the first cycle, a peak at 1.56 V appears, which is attributed to the formation of insoluble Li_2S_2 and Li_2S from small sulphur molecule S_{2-4} [5, 7]. In the second cycle, the cathodic peak shifts from 1.56 V to 1.62 V because of the formation of the complexes that have a lower absorbing energy after the initial cycle [11-13].

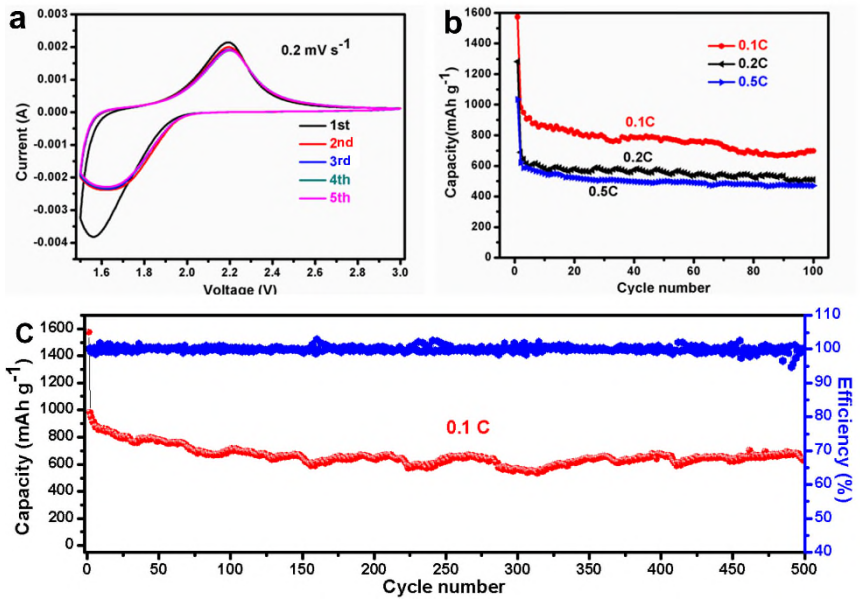

Fig. 4 (a) CV curves at a scanning rate of 0.2 mV s^{-1}. (b) The cyclic performance at different current densities. (c) The cyclic performance and coulombic efficiency at 0.1 C.

In the subsequent cycles, the CV curves almost overlap, which exhibits a high reversibility of NMCNFs/S cathodes. Fig. 4b exhibits the discharge capacity at various rates. The initial discharge capacities are 1573, 1282 and 1034 mAh g^{-1} under 0.1C, 0.2C and 0.5C, respectively. In the second cycle, the discharge capacities are dramatically decreased to 981, 688 and 622 mAh g^{-1}, respectively. These results may be attributed to the residual sulphur of not wrapped by micropores causing irreversible capacity loss after reaction with lithium. The specific capacity of NMCNFs/S cathodes was reduced when the discharge rate was increased, which illustrates that the low rate cycle is beneficial to achieving high specific capacity of micropores-confined sulphur materials. The coulombic efficiency (Fig. 3c) is stable and almost reaches to 100%, which indicates the excellent reaction reversibility for NMCNFs/S cathodes. Meanwhile, the NMCNFs/S cathode shows a stable cycle performance at 0.1C rate (after 500 cycles, the capacity still shows up to 636 mAh g^{-1}).

4 Conclusions

The obtained NMCNFs act as a binder-free sulphur host materials that show an excellent cycle stability and retain a high capacity of 636 mAh g^{-1} after 500 cycles because of its unique microstructure, high SSA (693 m^2 g^{-1}), nitrogen-doped and conductive nanofibre network. Overall, this work not only provides a design for high performance flexible binder-free cathode in lithium-sulphur batteries, but also suggests a facile synthesis method for the design of carbon nanofibres materials with micropores.

ACKNOWLEDGMENTS

This work was financially supported by the National Natural Science Foundation of China (No.51202150, 51272161,21703141), Program of Introducing Innovative Rese arch Team in Dongguan (No.2014607109)

Reference

[1] Z.W. Seh, Y. Sun, Q. Zhang, Y. Cui, Chem Soc Rev, (2016).
[2] A. Manthiram, Y. Fu, S.H. Chung, C. Zu, Y.S. Su, Chem Rev, 114 (2014) 11751-11787.
[3] P.G. Bruce, S.A. Freunberger, L.J. Hardwick, J.M. Tarascon, Nat Mater, 11 (2012) 19-29.
[4] X. Li, Y. Chen, H. Huang, Y.-W. Mai, L. Zhou, Energy Storage Materials, 5 (2016) 58-92.
[5] S. Niu, G. Zhou, W. Lv, H. Shi, C. Luo, Y. He, B. Li, Q.-H. Yang, F. Kang, Carbon, 109 (2016) 1-6.
[6] N. Jayaprakash, J. Shen, S.S. Moganty, A. Corona, L.A. Archer, Angew Chem Int Ed Engl, 50 (2011) 5904-5908.
[7] Z. Li, L. Yuan, Z. Yi, Y. Sun, Y. Liu, Y. Jiang, Y. Shen, Y. Xin, Z. Zhang, Y. Huang, Advanced Energy Materials, 4 (2014) -.
[8] S. Chu, Y. Zhong, R. Cai, Z. Zhang, S. Wei, Z. Shao, Small, 12 (2016) 6724-6734.
[9] H.J. Peng, T.Z. Hou, Q. Zhang, J.Q. Huang, X.B. Cheng, M.Q. Guo, Z. Yuan, L.Y. He, F. Wei, Advanced Materials Interfaces, 1 (2015).
[10] G. Zhou, E. Paek, G.S. Hwang, A. Manthiram, Nat Commun, 6 (2015) 7760.
[11] B. Zhang, X. Qin, G.R. Li, X.P. Gao, Energy & Environmental Science, 3 (2010) 1531.
[12] J.L. Wang, J. Yang, J.Y. Xie, N.X. Xu, Y. Li, Electrochemistry Communications, 4 (2002) 499-502.
[13] J. Wang, L. Lu, Z. Ling, J. Yang, C. Wan, C. Jiang, Electrochimica Acta, 48 (2003) 1861-1867.